Lattice Distortion, Polaron Conduction, and Jahn-Teller Effect on the Magnetoresistance of $La_{0.7}Ca_{0.3}MnO_3$ and $La_{0.5}Ca_{0.5}CoO_3$ Epitaxial Films

N.-C. Yeh[1], R. P. Vasquez[2], D. A. Beam[1], C.-C. Fu[1], H. Huynh[1], and G. Beach[1]

[1]Department of Physics, California institute of Technology, Pasadena, CA 91125

[2]Center for Space Microelectronics Technology, Jet Propulsion Laboratory, California Institute of 'Technology, Pasadena, CA 91109

Studies of $La_{0.7}Ca_{0.3}MnO_3$ epitaxial films on substrates with a range of lattice constants reveal that larger lattice distortion gives rise to larger zero-field resistivity and larger negative magnetoresistante. The colossal negative magnetoresistance (CMR) in the manganites at high temperatures ($T \to T_C$; T_C being the Curie temperature) is consistent with the hopping conduction of lattice polarons induced by the Jahn-Teller coupling, and the low-temperature ($T \ll T_C$) negative magnetoresistance is attributed to the magnetic domain wall scattering. In contrast, the absence of polar-on conduction in $La_{0.5}Ca_{0.5}CoO_3$ epitaxial films results in much smaller negative magnetoresistance.

Recent findings of colossal negative magnetoresistance (CMR) in the perovskite manganites $Ln_{1-x}A_xMnO_{3-\delta}$ (Ln: trivalent rare earth ions, A: divalent alkaline earth ions) have spurred intense research in the origin and further improvement of the magnetoresistance effects[1-7]. The perovskite manganites have been known for decades for their interesting magnetic phases and electronic properties as a function of the doping level (x)[8-12]. Upon increasing the doping level by substituting the Ln^{3+} ions with A^{2+}, the concentration of Mn^{4+} increases, giving rise to a mixture of Mn^{3+} and Mn^{4+} which initially yields canted spin configurations [10- 12] and then forms metallic bonding and ferromagnetism for the doping level of $0.2 \leq x \leq 0.4$[8- 12]. The occurrence of ferromagnetism has been attributed to the double-exchange interaction between Mn^{3+} and Mn^{4+} ions[8-12]. However, further theoretical investigations have revealed that the double-exchange alone cannot quantitatively account for the experimental observation, and that the strong electron-phonon interaction arising from the Jahn-Teller splitting may be important[6]. It is known that Mn^{3+} is a Jahn-Teller ion with a d-electron configuration $e_g^1 t_{2g}^3$ *which* contributes to the anisotropic magnetic properties due to the Jahn-Teller splitting of the outer d-orbitals of $d_{x^2-y^2}$ and *$d_{3z}z\_r2$[11].* The suggested relevance of the lattice effects on the conductivity and magnetism of these manganites is supported by increasing experimental evidence[3-5,7]. For instance, a strong correlation between the thickness of the epitaxial films and the corresponding magnetoresistance has been revealed in the $La_{0.7}Sr_{0.3}MnO_3$ system[3]. In addition, decreasing Curie temperatures and increasing CMR effects in the $La_{0.7-x}Ln'_x Ca_{0.3}MnO_3$ (Ln' $= Pr, Y, 0 \leq x \leq 0.7$) polycrystalline materials with the increasing lattice distortion have been demonstrated via the substitution of La ions by smaller ions of Pr and Y[4]. Another study on $La_{0.6}Pb_{0.4}MnO_3$ and $Nd_{0.6}(Sr_{0.7}Pb_{0.3})_{0.4}MnO_3$ single crystals has illustrated much smaller magnetoresistance as well as vanishing magnetoresistance for temperature $T \rightarrow 0$[5]. Moreover, a significant reduction of the magnetoresistance is observed in $Nd_{0.5}Sr_{0.36}Pb_{0.14}MnO_3$ single crystals under a hydrostatic pressure of 10.7 kbar[7].

To seek further understanding of the role of lattice distortion and Jahn-Teller effect on the occurrence of CMR, we report in this letter our experimental investigations of the transport and magnetic properties of $La_{0.7}Ca_{0.3}MnO_3$ and $La_{0.5}Ca_{0.5}CoO_3$ epitaxial films

on various perovskite substrates. The substrates selected include single crystalline $LaAlO_3$ (LAO), $SrTiO_3$ (STO), and $YAlO_3$ (YAO). As shown in Table I, these substrates are chosen to provide a range of lattice constants which allows studies of the effects of tensile and compressive stress of the films. By maintaining the same chemical composition, oxygen annealing condition, and film thickness for all samples, we can investigate the net effect of lattice distortion on the transport and magnetic properties. On the other hand, to investigate the relevance of the Jahn-Teller coupling, we consider the cobaltites $La_{1-y}Ca_yCoO_3$ which are known to be highly conductive ferromagnets at doping levels of $0.4 < y \leq 0.6$[11,13]. In these cobaltites, the Co^{3+} and Co^{4+} ions are known to exist in the form of both the high-spin and low-spin states, so that the d-electron configurations may assume either $e_g^0 t_{2g}^6$ (low-spin) or $e_g^2 t_{2g}^4$ (high-spin) states for the Co^{3+} ions, and for the Co^{4+} ions either $e_g^0 t_{2g}^5$ (low-spin) or $e_g^2 t_{2g}^3$ (high-spin) states[11]. The coexistence of cobalt ions with either entirely empty or half-filled e_g orbitals is essential for high electrical conductivity and ferromagnetism in these cobaltites. However, neither the empty nor the half-filled e_g orbitals yield any Jahn-Teller effect. Therefore the controlled comparison of the magnetoresistance of the cobaltites with that of the manganites may provide further insights into the correlation of CMR with the Jahn-Teller effect.

The $La_{0.7}Ca_{0.3}MnO_3$ (LCMO) and $La_{0.5}Ca_{0.5}CoO_3$ (LCCO) epitaxial films are grown by pulsed laser deposition using stoichiometric targets of $La_{0.7}Ca_{0.3}MnO_3$ and $La_{0.5}Ca_{0.5}CoO_3$. The films are grown in 100 mTorr of oxygen with the substrate temperature at $700°C$, and subsequently annealed at $900°$ C of 1 atm oxygen for two hours. The oxygen concentration is believed to be stoichiometric because any longer annealing time does not yield further increase of the Curie temperature T_C, and the T_C values for both LCMO ($T_C = 260 \pm 5$ K) and LCCO ($T_C = 180 \pm 5$ K) are consistent with those for the bulk material. The thickness of all samples is 200+ 10 nm, and the lattice constants a, b and c (c $\perp$ sample surface) as well as the epitaxy of the films are determined using high resolution x-ray diffraction spectroscopy and x-ray rocking curves. The results are tabulated in Table 1. The chemical properties of these samples were further characterized with x-ray photoelectron spectroscopy (XPS)[14]. The results indicate that no interdiffusion takes place between the substrate material and

the film except for LCCO/STO. Further-more, no density of states at the Fermi level was observed for the manganites[14], consistent with the semiconducting nature of these samples at room temperature. In contrast, a high density of states at the Fermi level is observed for the cobaltites[14], in agreement with the metallic nature ($\rho \leq 10^{-4}\Omega$ cm at 300 K) of these materials.

The physical properties of both the manganites and cobaltites are studied via measurements of the resistivity and magnetization. The dimensions of the samples are 2mm x 2mm x 200nm, and the standard four-probe measurements are performed by making contact to sputtered gold electrodes. The resistivity is measured in a magnetic field varying from O to 6 Tesla, and the anisotropic magnetoresistance is studied by varying the orientation of the magnetic field from O to 90° relative to the sample surface. The applied current is always along one axis of the sample and is transverse to the external field. The magnetic field and temperature dependence of the resistivity is found to be comparable for all field orientations, although the quantitative details differ slightly due to the existence of a small magnetic anisotropy. The magnetization measurements are performed using a SQUID magnetometer by Quantum Design, with the applied field parallel to the sample surface.

The lattice distortion induced by the substrates yields two effects which are relevant to our consideration. One is the lattice strain, defined as $(\Delta a_0 / a_o)$, where a_0 is the lattice constant of the bulk perovskite, and Au. is the difference between the lattice constant of the film and that of the bulk. The other is the lattice relaxation between the substrate and the film, defined as (As,/a.), where a_s is the lattice constant of the substrate, and Δa_s is the difference between the lattice constant of the film and that of the substrate. We note that for films thicker than a critical thickness, the epitaxial films may acquire lattice constants different from those of the substrates, thereby giving rise to "extrinsic" distortion such as dislocations and domains. On the other hand, the lattice strain is an indicator of the more intrinsic distortion in properties such as the magnetic exchange interactions and electron-phonon interaction. These two types of lattice distortion induced by three different substrates are listed in Table 2 for both LCMO and LCCO films. We note that among LCMO films, the lattice strain for the a and b axes is tile largest in I, CMO/STO, and the lattice relaxation

is the largest in LCMO/YAO. On the other hand, for LCCO films, although no significant lattice distortion occurs in the LCCO/LAO sample, the lattice relaxation is significant in LCCO/YAO.

Next, we consider the effects of lattice distortion on the resistivity and magnetoresistance of the fully oxygenated LCMO films. As illustrated in Figs. 1 (a)–(c), the largest lattice distortion in the LCMO/YAO film yields the highest zero-field resistivity $\rho(H = 0, T)$ and the largest magnetoresistance AR_H at $H = 60$ kOe. Here we define the magnetoresistance in a magnetic field H as $\Delta R_H \equiv [\rho(H) - \rho(0)]/\rho(H)$. Comparing the lattice distortion of LCMO/LAO and LCMO/STO, we note that the latter has a larger tensile strain, though smaller lat t ice relaxation. This tensile strain may reduce the in-plane Mn-O-Mn exchange interaction, yielding less favorable ferromagnetic coupling[15] anti possibly larger resistivity and enhanced negative magnetoresistance.

In Figs.2(a)-(c), some representative resistivity data as a function of the magnetic field at various constant temperatures are shown for the annealed I. CMO/LAO, LCMO/YAO and I. CMO/STO films. We note that the ρ-vs.-H isotherms are monotonically decreasing with H for all samples, and those for the least distorted LCMO/LAO are the smoothest. On the other hand, for both LCMO/STO and LCMO/YAO films, some isotherms exhibit a distinct change in the slope. To obtain a better understanding of the temperature and magnetic field dependence of the resistivity, wc consider a mechanism based on polaron conduction [5,6]. Assuming dominant polaron hopping conduction at high temperatures, we obtain the fitting curves shown as the solid lines in Figs. 1 and 2 by using the following formulae:

$$\rho(T) \approx \frac{\alpha T}{(1 + G)} \exp\left[\frac{E_b(T)}{k_B T}\right] \equiv \frac{\alpha T}{(1 + G)} \exp\left\{\frac{E_{b0}}{k_B T} [1 - G(T)]\right\},$$

$$p(H) \approx \frac{\alpha T}{(1 + G')} \exp\left[\frac{E_b(H)}{k_B T}\right] \equiv \frac{\alpha T}{(1 + G')} \exp\left\{\frac{E_{b0}}{k_B T} [1 - G'(H)]\right\}, \tag{1}$$

where E_b is the polaron binding energy, α a constant, G(T) and $G'(H)$ arc empirically determined functions closely related to the normalized magnetization $m \equiv (M/M_s)$, with $M(H, T)$ being the magnetization and M_s the saturation magnetization, Using Eq.(1) and the functions of G(T) and $G'(H)$ given in Figs.3(a) and 3(b), the polaron model yields the same fitting

parameter $E_{b0} \approx 0.35$ CV for all LCMO films on different substrates, as shown by the solid lines in Figs.1 and 2. We note the close correlation of $G(T)$ and $G'(H)$ with the experimental magnetization data $M(T)$ and $M(H)$, as illustrated in Figs.3(a) and 3(b). Furthermore, $G(T) \to ?72(7') \approx 1$ for $T \ll T_C$, and $G \to 0$ for $T \gg T_C$. Similarly, $G'(H) \to m(H) \approx 1$ for large H, and $G'(H) \to O$ for $H \to O$. The correlation of G and G' with the magnetization strongly suggests the important role of magnetic ordering in the electrical conduction. We also note that by replacing G with m, our generalized form in Eq.(1) recovers the simplified expression for polaron conduction in Ref. [5], and $E_b \to O$ for $m \to 1$, consistent with complete unbinding of polarons in the limit of complete magnetic ordering. The relatively large polaron binding energy ($E_{b0} \approx 0.35$ eV) derived from the use of Eq.(1) may be compared with the Jahn-Teller energy of ~ 0.5 CV for undoped $LaMnO_3$ [4]. Considering the 30% decrease of the Mn^{3+} Jahn-Teller ions in our LCMO samples, the derived polaron binding energy appears consistent with the formation of lattice polarons[4], r-tither than magnetic polarons due to the electron-spin interaction[16].

Comparing the $M(T)$ data of all LCMO films and that of the bulk, we note that the slower rise of magnetization below T_C for samples of larger lattice distortion appears to be correlated with larger resistivity and magnetoresistance. This observation is consistent with the formation of lattice distortion-induced magnetic domains. Although all domains undergo a ferromagnetic phase transition at the same temperature, below T_C the incompletely aligned "superparamagnetic" moments of the magnetic domains in samples with larger lattice distortion gives rise to slower rising magnetization and larger scattering of conduction electrons. Therefore the application of external magnetic. fields has more significant effects on aligning the magnetic domains and reducing the resistivity in samples with larger lattice distortion.

As manifested in Fig.1, the scenario of magnetic domain wall scattering is consistent with the finite resistivity and magnetoresistance at low temperatures where the polaron contribution vanishes. Furthermore, the distinct change of slope in the low-temperature ρ-vs.-H isotherms (see Fig.2) also indicates changes in the scattering mechanism, To further verify the presence of magnetic domain wall scattering, we note that for the least distorted samples of LCMO/LAO, the ρ-vs.-H isotherms over a large magnetic field range can be consistently

described by the field dependence given in Eq.(1). On the other hand, for the LCMO/STO and LCMO/YAO, samples with larger lattice distortion, only the higher field portion of the data can be described by Eq. (1). This phenomenon may be understood in terms of the better alignment of magnetic domains in higher fields so that the domain wall scattering is reduced.

To further distinguish the resistivity contribution due to the domain wall scattering from that due to the lattice polarons, the resistivity and magnetization of fully oxygenated $La_{0.5}Ca_{0.5}CoO_3$ epitaxial films on LAO and STO substrates were studied. As pointed out earlier, the cobaltites were chosen because of the absence of the Jahn-Teller effect in these samples. Despite comparable lattice relaxation and lattice strain in both the manganites and cobaltites, as shown in Tables 1 and 2, the magnitude anti temperature dependence of the resistivity in these two systems exhibit sharp contrasts, as illustrated in Figs.1(a)-(c) and Figs.4(a)-(b). The resistivity of the cobaltites may be understood in terms of the combination of conventional impurity, phonon, and disorder-spin scattering. As shown in Fig.4, for both LCCO/LAO and LCCO/YAO samples, the temperature below which a faster decrease in the zero-field resistivity occurs coincides with the Curie temperature $T_c \approx 180$ K, suggesting that magnetic ordering below T_C reduces the resistivity. It appears that the absence of polaron conduction in the cobaltites may be responsible for the much smaller magnitude of negative magnetoresistance.

In summary, we have investigated the role of lattice distortion, polaron conduction and Jahn-Teller coupling in the occurrence of the colossal negative magnetoresistance in perovskite oxides. By comparing the electrical transport and magnetic properties of $La_{0.7}Ca_{0.3}MnO_3$ films on substrates with different lattice constants, we conclude that larger lattice distortion gives rise to larger zero-field resistivity and larger magnitude of negative magnetoresistance. The colossal negative magnetoresistance at high temperatures has been attributed to the conduction of lattice polarons, because that the polaron binding energy ~ 0.35 eV is comparable to the Jahn-Teller energy, and that the resistivity is closely correlated with the magnetization. On the other hand, the low-temperature magnetoresistance is found to be consistent with the magnetic domain wall scattering. We have also studied the magnetotransport properties of the highly conductive cobaltites $La_{0.5}Ca_{0.5}CoO_3$ with lattice distortion comparable

in $La_{0.7}Ca_{0.3}MnO_3$, and found that lattice distortion alone is insufficient to yield colossal negative magnetoresistance. We therefore conclude that the conduction of lattice polarons associated with the Jahn-Teller coupling in the manganites is essential for the occurrence of the colossal negative magnetoresistance, and that lattice distortion further enhances the negative magnetoresistance.

REFERENCES

[1] R. von Hemlolt et al., Phys. Rev. Lett. 71, 2331 (1993).

[2] H. L. Jue tal., Appl. Phys. Lett. 65, 2108 (1994); Phys. Rev. B51, 6143 (1995).

[3] S. Jin et al., Science 264, 413 (1994); Appl. Phys. Lett. 66, 382 (1995); Appl. Phys. Lett. 67, 557 (1995).

[4] H. Y. Hwang et al., Phys. Rev. Lett. 75, 914 (1995).

[5] Y. X. Jia et al., Phys. Rev. B52, 9147 (1995).

[6] A. J. Minis, P. B. Littlewood, and B. I. Shraiman, Phys. Rev. Lett. 74, 5144 (1995).

[7] K. Khazeni et al., Phys. Rev. Lett. 76, 295 (1996).

[8] G. H. Jonker and J. H. van Santen, Physica 16, 337 (1950); J. H. van Santen and G. H. Jonker, Physica 16, 599 (1950).

[9] C. Zener, Phys. Rev. 82, 403 (1951).

[10] E. O. Wollan and W. C. Koehler, Phys. Rev. 100, 545 (1955).

[11] J. B. Goodenough, Phys. Rev. 100, 564 (1955); in *"Progress in Solid State Chemistry"*, Vol. 5, Pergamon Press (1971), ed. by H. Reiss.

[12] P. G. deGennes, Phys. Rev. 118, 141 (1960).

[13] H. Ohbayashi, T. Kudo and T. Gejo, Jpn. J. Appl. Phys. 13, 1 (1974).

[14] R. P. Vasquez et al., (unpublished).

[15] V. A. Bokov et al., Phys. Stat. Sol. 28, 835 (1968).

[16] R. M. Kusters et al., Physics 13155, 362 (1989).

Table 1 The lattice constants determined from x-ray diffraction for $La_{0.7}Ca_{0.3}MnO_3$ (LCMO) and $La_{0.5}Ca_{0.5}CoO_3$ (LCCO) epitaxial films on substrates of $LaAlO_3$ (LAO), $YAlO_3$ (YAO), and $SrTiO_3$ (STO). The lattice constants for bulk LCMO and LCCO and those for the substrates are also listed.

Compound	Lattice constant $(Å)$		
	$(a/\sqrt{2})$	$(b/\sqrt{2})$	$(c/2)$
LCMO	3.840	3.890	3.860
LCCO	$a=3.792$		
LAO	$a=3.792$		
YAO	3.662	3.768	3.685
STO	$a=3.905$		
I, CMO/LAO	3.842	3.854	3.921
LCMO/YAO	3.862	3,886	3.899
I, CMO/STO	3.881	3.927	3.845
LCCO/LAO	3.790	3.790	3.793
LCCO/YAO	3.828	3.823	3.777

Table 2 The comparison of the lattice relaxation and lattice strain for LCMO and LCCO epitaxial films on substrates of LAO, YAO and STO.

Compound	Lattice Relaxation (%)			Lattice Strain (%)		
	$\dfrac{\Delta a_{\parallel}}{a}$	$\dfrac{\Delta b}{b}$	$\dfrac{\Delta c}{c}$	$\dfrac{\Delta a_0}{a_0}$	$\dfrac{\Delta b_0}{b_0}$	$\dfrac{\Delta c_0}{c_0}$
LCMO/LAO	1.32	1.64	3.40	0.05	-0.93	-' 1.58
LCMO/YAO	4.80	3.08	5.66	0.57	-0.10	1.01
LCMO/STO	0.62	0.56	1.40	1.07	0.95	-0.39
LCCO/LAO	-0.05	-0.05	0.03	-0.05	-0.05	0.03
I, CCO/YAO	4.50	1.41	2.35	0.95	0.82	-0.40

Fig.1 The effect of lattice distortion on the resistivity of $La_{0.7}Ca_{0.3}MnO_3$ (for both $H = 0$ and $H = 60\,kOe$) for oxygen-annealed epitaxial films on different substrates: (a) $LaAlO_3$, (b) $YAlO_3$, and (c) $SrTiO_3$. The corresponding magnetoresistance (ΔR_H) vs. temperature (T) data are shown in the insets, and the solid lines are fitting curves using Eq.(1).

Fig.2 The magnetic field dependence of the resistivity $(\rho$ vs. $H)$ at various constant temperatures for **(a)** LCMO/LAO, **(b)** LCMO/YAO and (c) LCMO/STO epitaxial films. The solid lines are fitting curves using Eq.(1) over the range of fields in which the expression is applicable.

Fig.3 (a) The temperature dependence of the correlation function $G(T)$ for I, CMO/LAO, LCMO/STO and LCMO/YAO films (the solid lines) for both $H = 0$ and $H = 60$ kOe. The inset shows the temperature dependence of the magnetic moments $M(T)$ for LCMO/LAO, LCMO/STO and I. CMO/YAO films and bulk LCMO taken at $H = 6$ kOe. Note the much faster saturation of $M(T)$ below T_C for bulk LCMO relative to that of the films. (b) The representative $G'(H)$ -vs.-H isotherms for the LCMO/LAO film. The corresponding M-vs.-H data are shown in the inset.

Fig.4 The effect of lattice distortion on the resistivity of $La_{0.5}Ca_{0.5}CoO_3$ (for both $H = 0$ and $H = 60\,kOe$) for oxygen-annealed epitaxial films on different substrates: **(a)** $LaAlO_3$; **(b)** $YAlO_3$. The corresponding magnetoresistance (ΔR_H) vs. temperature (T) data as well as the M-vs.-T curve are shown in the insets.

Figure 1
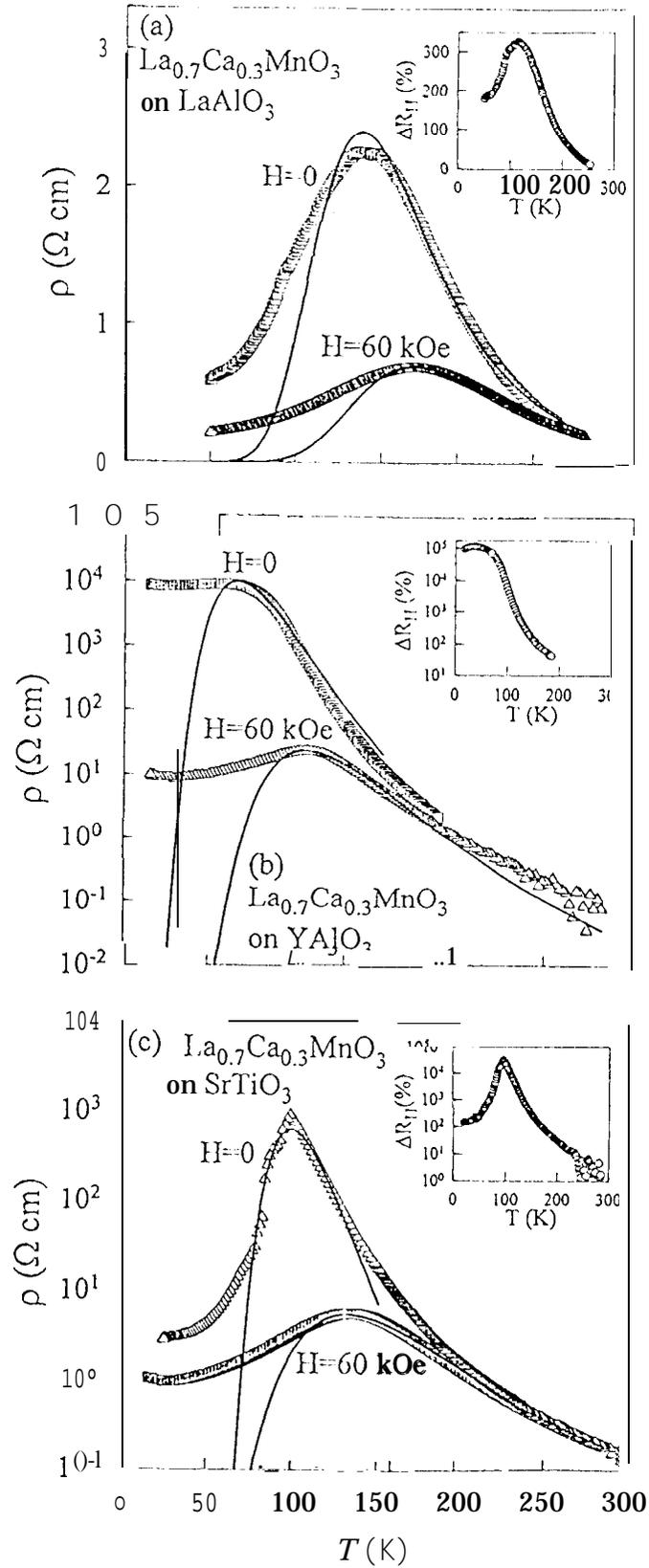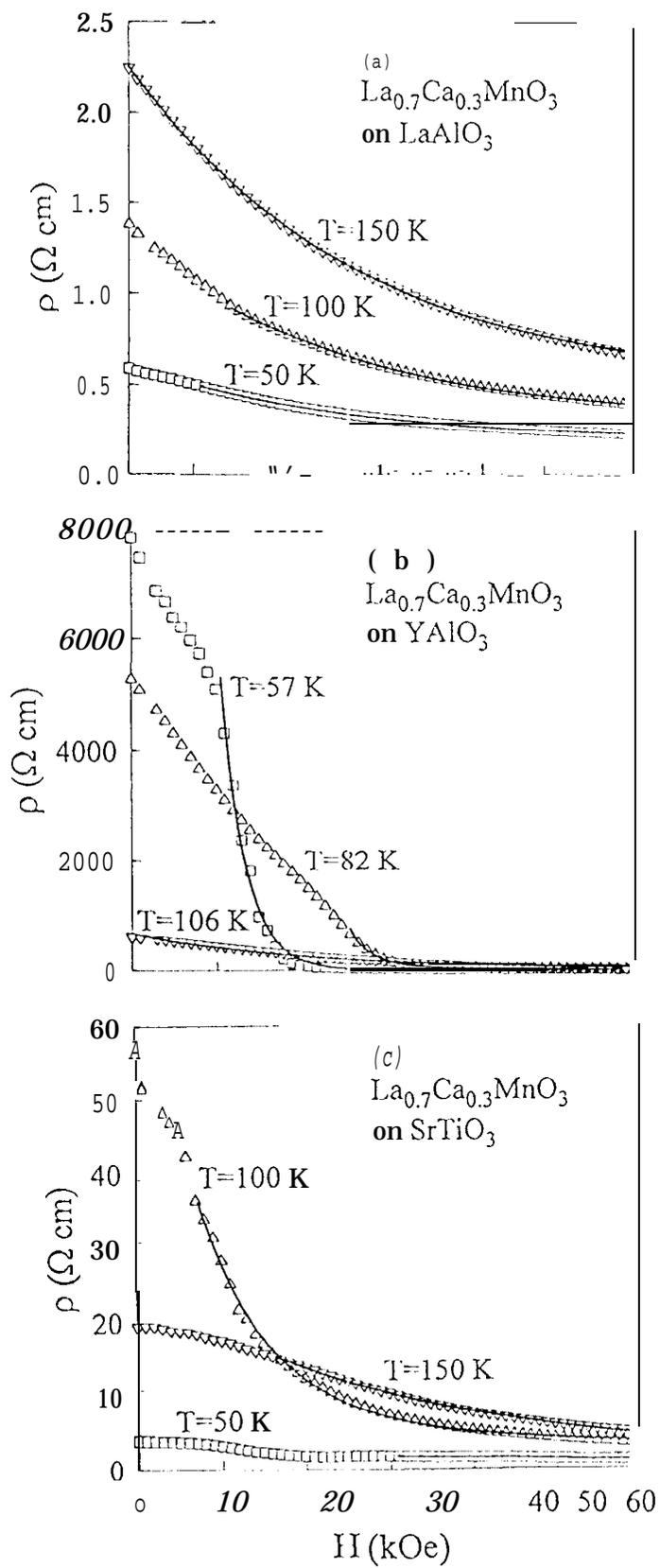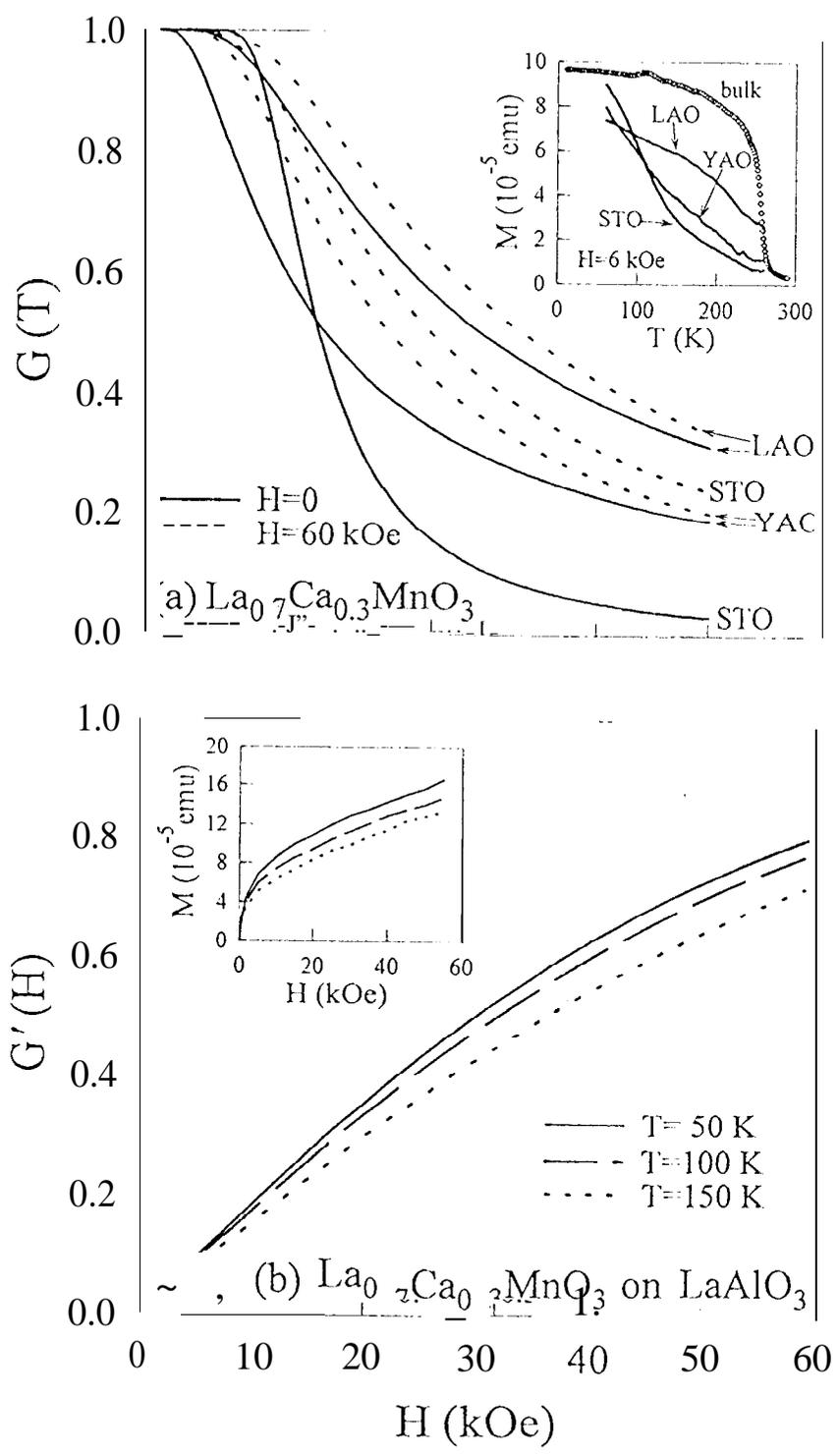
(a)
$La_{0.7}Ca_{0.3}MnO_3$
on $LaAlO_3$

$T=150$ K

$T=100$ K

$T=50$ K

(b)
$La_{0.7}Ca_{0.3}MnO_3$
on $YAlO_3$

$T=57$ K

$T=82$ K

$T=106$ K

(c)
$La_{0.7}Ca_{0.3}MnO_3$
on $SrTiO_3$

$T=100$ **K**

$T=150$ K

$T=50$ **K**

H (kOe)

Figure 2

Figure 3

a. $_5Ca_{0.5}CoO_3$ on $LaAlO_3$

(b) $La_{0.5}Ca_{0.5}CoO_3$ on $YAlO_3$

Figure 4